Investigation of Sub-Cell Homogenization for PHWR Lattice Cells using Superhomogenization Factors

By

Subhramanyu Mohapatra

A Thesis Submitted in Partial Fulfillment
of the Requirements for the Degree of
Master of Applied Science
in

The Faculty of Energy Systems and Nuclear Science

Nuclear Engineering

University of Ontario Institue of Technology

December, 2016

Abstract

To avoid the computational effort associated with full-core neutron transport calculations, full-core neutronics calculations for Pressurized Heavy-Water Reactors (PHWRs) are usually performed in diffusion theory using an approximate core model, whereby only two energy groups are utilized and two-group neutronic properties (i.e. macroscopic cross sections and diffusion coefficients) are homogenized in two dimensions over large sub-domains, each corresponding to a 28.6 cm x 28.6 cm *lattice cell*. The lattice cell is the elementary geometrical unit describing the rectangular array of fuel channels comprising the PHWR core. The use of lattice-cell homogenization introduces some computational errors. One possible way to reduce such homogenization errors is to sub-divide the lattice cell into sub-cells and perform sub-cell-level homogenization. In this study, the PHWR lattice cell is divided into 3 x 3 sub-cells. Full-cell-averaged, as well as sub-cell-averaged two-group cross-sections, are generated for subsequent use in an equivalent two group two-dimensional diffusion model. Cross sections with Superhomogenization (SPH) [Hebert, 2009] factors are also utilised in an attempt to improve accuracy. The effect of using different homogenization models (full cell, partial cell, partial-cell with SPH-corrected cross sections) is tested on a two-dimensional partial-core model consisting of 3 x 3 lattice cells (bundles). Results from reference transport model with detailed geometry 69-group are compared with cell-homogenized two-group diffusion results obtained using full-cell homogenization and sub-cell homogenization with and without SPH correction factors. The application of sub-cell homogenization, as well as the use of SPH correction factors, is found to have only a minimal effect on computational accuracy.

Keywords: Applied Reactor Physics, Superhomogenization, PHWR, SPH Factors

Acknowledgements

I would sincerely like to thank my supervisor, Dr Eleodor Nichita. His guidance, encouragements and knowledge made this work possible. Thank you for the motivation you gave me to finish this work.

I would also like to thank Peter Schwanke and Jawad Haroon for their help in learning concepts of the reactor physics and computational tools. To them, my gratefulness will always fall short.

Last but certainly not least, I would like to offer my heartiest thanks to my parents, my wife and my friends for their encouragement and support throughout the different stages of this effort.

Table of Contents

Chapter 1: Introduction 1

1.1. Neutron Transport Equation 1

1.2. Neutron Diffusion Equation 5

1.3. Thesis outline 8

Chapter 2: Problem Statement 10

2.1. Introduction 10

2.2. Standard Homogenization 10

2.3. Problems with Standard Homogenization 13

Chapter 3: Progress to date in PHWR Homogenization 14

Chapter 4: Method 19

4.1. Theoretical background 19

4.1.1. Sub-cell homogenization 19

4.1.2. Superhomogenization 20

4.2. Computational Tools 21

4.2.1. DRAGON 22

4.2.2. DONJON 22

4.2.3. DRAGON/DONJON Code-Input Structure 23

4.2.4. Modules 24

4.3. Calculation Steps 24

4.4. SPH factor generation in DRAGON 26

Chapter 5: Models 27

5.1. Lattice Cell Models 27

5.1.1. DRAGON Lattice cell model 28

5.1.2. DONJON lattice cell model 34

5.2. Partial core models 34

5.2.1. Reference Partial Core Model 35

5.2.2. Partial Core DONJON Models 36

Chapter 6: Results and Discussion 39

6.1. Flux Normalisation 39

6.2. Lattice cell results 40

6.3. Lattice cell results interpretation 41

6.4. Partial-Core Results 42

6.5. Partial-core results interpretation 46

6.6. Discussion 47

Chapter 7: Summary, Conclusion and Future Work 50

7.1. Summary 50

7.2. Conclusion 51

7.3. Future Work 51

References 53

List of Figures

Figure #	Description	Page #
Figure 2.1	A typical 2D PHWR lattice cell.	11
Figure 2.2	Pictorial representation of the standard homogenization method applied in PHWR	12
Figure 4.1	Schematic representation of sub-cell homogenization in PHWR fuel channels.	20
Figure 4.2	Schematic of the input file structure for DRAGON/DONJON	23
Figure 4.3	Methodology flow chart.	26
Figure 5.1	PHWR Lattice cell model generated using DARGON 3.05. Colours represent different materail mixtures	29
Figure 5.2	Spatial discretization applied in DRAGON lattice cell.	30
Figure 5.3	Fine spatial discretization at fuel pin level in the lattice cell model.	31
Figure 5.4	Diagram of the data flow in the DRAGON lattice cell model	33
Figure 5.5	DONJON lattice cell model. Each colour represents a different set of homogenized cross sections	34
Figure 5.6	3×3 Partial core reference model designed in DRAGON ZB represents zero burnup sections, and DB represents discharge burnup.	36
Figure 5.7	Partial core DONJON model with Standard Homogenization. Each colour represents a different set of homogenized cross sections	37
Figure 5.8	DONJON partial core model sub-cell homogenization with 81 regions. Each colour represents a different set of homogenized cross sections	38
Figure 5.9	DONJON partial core model sub-cell homogenization with 144 regions. Each colour represents a different set of homogenized cross sections	38

List of Tables

Table #	Description	Page #
Table 6.1	Normalised fluxes and % error for the lattice cell without using SPH factors (arbitrary units)	40
Table 6.2	Normalised fluxes for the lattice cell with using SPH factors (arbitrary units) % error is zero in all cases	41
Table 6.3	k-eff and normalised fission rates for type K calculations of partial core reference model	43
Table 6.4	k-eff and normalised fission rates for type B calculations of partial core reference model	43
Table 6.5	k-eff and normalised fission rates of partial core DONJON model with standard homogenization.	43
Table 6.6	k-eff and normalised fission rates of partial core DONJON model for sub-cell homogenization (a) with SPH factors (b) without SPH factors for 81 region splitting	44
Table 6.7	k-eff and normalised fission rates of partial core DONJON model for sub-cell homogenization (a) with SPH factors (b) without SPH factors for 144 region splitting	44
Table 6.8	k-eff and normalised fission rate errors in 81regions and144 regions w.r.t reference model with type K calculations	45
Table 6.9	k-eff and normalised fission rate errors in 81regions and144 regions w.r.t reference model with type B calculations	46
Table 6.10	Percentage error in thermal SPH factors in partial core model (81 regions) with respect to single lattice model.	48

List of Symbols

D_2O	Deuterium oxide (heavy water)
E	Energy
k_{eff}	Multiplication constant
MWd/t(U)	Megawatt days per metric tonne of uranium fuel mass
mk	Mesurment for multiplication constants (0.001k)
V_r	Volume for a fine region in lattice cell
V_R	Volume for a coarse region in lattice cell
UO_2	Uranium dioxide
χ	Fission Spectrum
Ψ	Heterogeneous Flux
Φ	Homogenous Flux
$\hat{\Omega}$	Solid angel for neutron direction
ϕ	Intergral neutron flux
Σ_t	Macroscopic cross section for total removal
Σ_s	Macroscopic cross section for scattering
Σ_f	Macroscopic cross section for fission
μ	Superhomogenization Factor
ν	Total neutron yields per fission

List of Acronyms

ACMFD	Analytic Coarse Mesh Finite Difference
ADF	Assembly Discontinuity Factor
AECL	Atomic Energy Canada Limited
BWR	Boiling Water Reactor
GET	Generalised Equivalence Theory
LWR	Light Water Reactor
MOX	Mixed Oxide
PHWR	Pressurized Heavy Water Reactor
PWR	Pressurized Water Reactor
RFSP	Reactor Fueling Simulation Program
SPH	Superhomogenization
WIMS	Winfrith Improved Multi-group Scheme
WLUP	WIMS Library Update Project

Chapter 1: Introduction

Neutronics calculations carried out for the design and operation of thermal nuclear reactors usually proceed in two steps: a lattice-level step, and a core-level step. The core-level step utilises large-region-averaged neutronic properties generated by the lattice-level calculations. The generation of such average cross sections is called homogenization. Most aspects of the homogenization calculations are common to both Pressurized Water Reactors (PWRs) and Pressurized Heavy-Water Reactors (PHWRs), but specific features also exist. This study is focused on homogenization techniques for PHWRs.

The following sections explain the neutron transport equations and diffusion equations used to model the reactor core, and subsequently, the description of homogenization related errors are presented.

1.1.Neutron Transport Equation

The neutron transport equation is the most accurate representation of the behaviour of neutron population in the nuclear reactor core. It is based on several assumptions. Firstly, the relativistic effects can be neglected as maximum neutron speeds achieved in a nuclear reactor are less than $1/10^{th}$ of the speed of light. Secondly, to keep the equation linear, only neutron collisions with nuclei are considered, while neutron-neutron collisions are ignored, as the neutron density is several orders of magnitude smaller than the atom density of materials in a reactor. Finally, neutron paths between collisions are assumed to be straight lines [Hebert, 2009]. Equation (1.1) shows the continuous-energy transport equation which expresses the neutron balance equation for any arbitrary infinitesimal volume.

$$\frac{\partial n(\vec{r},E,\hat{\Omega},t)}{\partial t} = -\hat{\Omega}\cdot\nabla\psi(\vec{r},E,\hat{\Omega},t) - \Sigma_t(\vec{r},E,t)\psi(\vec{r},E,\hat{\Omega},t)$$
$$+\int_0^{\infty}\int_{4\pi}\Sigma_s(\vec{r},E'\to E,\hat{\Omega}'\to\hat{\Omega},t)\psi(\vec{r},E',\hat{\Omega}',t)d\hat{\Omega}dE' + \frac{\chi(E)}{4\pi}\int_0^{\infty}\nu(E')\Sigma_f(\vec{r},E',t)\psi(\vec{r},E',t)dE' \quad (1.1)$$
$$+ s(\vec{r},E,\hat{\Omega},t)$$

Equation (1.1) is called the integro-differential form of the neutron-trsanspoirt equation because it is a partial differential equation with respect to spatial variables and, at the same time, an integral equation with respect to the energy and angle variables. The term on the left side represents the rate of change of angular neutron density with respect to time. $\psi(\vec{r},E,\hat{\Omega},t)$ represents the angular flux as a function of position, energy, solid angle and time. $\Sigma_t(\vec{r},E,t)$ is the macroscopic total removal cross section. $\Sigma_s(\vec{r},E'\to E,\hat{\Omega}'\to\hat{\Omega},t)$ represents the down-scattering into the energy interval dE from the energy interval dE'. $\chi(E)$ is the normalised fission neutron energy distribution. $\nu(E')$ is the total neutron yield as a function of energy. $\Sigma_f(\vec{r},E',t)$ is the macroscopic fission cross section and $\psi(\vec{r},E',t)$ represents the total neutron flux, as the fission reaction is independent of the direction of neutrons in the target volume, there is no argument of solid angle in the above flux function.

The first term on the right side of the equation (1.1) is shown separately in equation (1.2); it represents the loss of neutrons due to leakage from an infinitesimal volume , which leads to a negative sign before it.

$$\text{Loss by leakage} = \hat{\Omega}\cdot\nabla\psi(\vec{r},E,\hat{\Omega},t) \quad (1.2)$$

The second term on the right side of the equation (1.1) is shown separately in equation (1.3) below; it represents the loss of neutrons due to nuclear interactions such as absorption and scattering.. It is also referred to as the total removal rate, and a negative sign also precedes it.

$$Total\_removal\_rate = \Sigma_t(\vec{r}, E, t)\psi(\vec{r}, E, \hat{\Omega}, t) \tag{1.3}$$

The third term on the right side of the equation (1.1) is represented separately in equation (1.4); it shows the neutrons gained due to scattering interactions of neutrons in an infinitesimal volume and a positive sign precedes it.

$$neutrons\_gain\_due\_to\_scattering = \int_0^\infty \int_{4\pi} \Sigma_s(\vec{r}, E' \to E, \hat{\Omega}' \to \hat{\Omega}, t)\psi(\vec{r}, E', \hat{\Omega}', t)d\hat{\Omega}dE' \tag{1.4}$$

The fourth term in Equation (1.1) represents the neutron generation from fission reactions. It is shown separately in equation (1.5), and a positive sign precedes it.

$$neutrons\_from\_fission = \frac{\chi(E)}{4\pi}\int_0^\infty \nu(E')\Sigma_f(\vec{r}, E', t)\psi(\vec{r}, E', t)dE' \tag{1.5}$$

Finally, the last term represents an external (independent of the flux level) neutron source and is preceded by a positive sign.

The leakage term, equation (1.2), includes the gradient of the angular flux. The scattering term shown in equation (1.4) has two integrals, one over the solid angle 4π and another over the energy spectrum. The fission neutrons source term shown in equation (1.5) has one integral over the energy range. All these constitute a complex integrodifferential form of the neutron transport equation.

Some fundamental problems like initial designs, reactivity device worth associated with the reactor physics can be solved considering the steady-state case. For these time-independent problems, the time-independent, the neutron balance equation simplifies to the form in equation (1.6).

$$\hat{\Omega}\cdot\nabla\psi(\vec{r},E,\hat{\Omega})+\Sigma_t(\vec{r},E)\psi(\vec{r},E,\hat{\Omega})=$$
$$\int_0^\infty\int_{4\pi}\Sigma_s(\vec{r},E'\to E,\hat{\Omega}'\to\hat{\Omega})\psi(\vec{r},E',\hat{\Omega}')d\hat{\Omega}dE'+\frac{1}{k}\frac{\chi(E)}{4\pi}\int_0^\infty\nu(E')\Sigma_f(\vec{r},E')\psi(\vec{r},E')dE' \quad (1.6)$$

The production term is divided by a constant "*k*", called the "effective multiplication constant", in order to force equality between the production rate and the loss rate. Additionally, all the nuclear reactions depend on the neutron's energy involved in the interactions and neutron energy spectrum in a reactor spans a wide range, from meV to MeV. For numerical computations, the neutron energy range is divided into multiple "energy groups", a process called energy discretization [Hebert, 2009]. The multi-group neutron balance transport equation is given in equation (1.7).

$$\nabla\cdot[\hat{\Omega}\psi_g(\vec{r},\hat{\Omega})]+\Sigma_{tg}(\vec{r},\hat{\Omega})\psi_g(\vec{r},\hat{\Omega})=$$
$$\sum_{g'}\int_\Omega\Sigma_{g'\to g,\hat{\Omega}'\to\hat{\Omega}}(\vec{r})\psi_{g'}(\vec{r},\hat{\Omega})d\Omega'+\frac{1}{k}\frac{\chi_g}{4\pi}\sum_{g'}\int_{\Omega'}\Sigma_{fg'}(\vec{r})\psi_{g'}(\vec{r},\Omega')d\Omega' \quad (1.7)$$

where $\psi_g(\vec{r},\hat{\Omega})$ is the condensed flux in group g, $\Sigma_{tg}(r,\hat{\Omega})$ is the total removal cross sections from group g, $\Sigma_{g'\to g,\hat{\Omega}'\to\hat{\Omega}}(\vec{r})$ is the scattering cross section.

Furthermore, the neutron current can be defined as

$$\vec{J}_g(\vec{r})=\int_\Omega\hat{\Omega}\psi_g(\vec{r},\hat{\Omega})d\Omega \quad (1.8)$$

Because reaction rates do not depend on the incident neutron flux's direction, it is useful to define the integral group flux as

$$\phi_g(\vec{r})=\int_\Omega\psi_g(\vec{r},\hat{\Omega})d\Omega \quad (1.9)$$

In the first leakage component after taking the divergence operator outside, the product term of the solid angle and the group flux can be simplified by substituting it with the current term as per equation (1.8). Moreover, the flux appearing in the source terms can be substituted by equation (1.9). Equation (1.10) represents the multi-group neutron balance equation with the current and integral flux in the source term.

$$\nabla \cdot \vec{J}_g(\vec{r}) + \Sigma_{tg}(\vec{r})\phi_g(\vec{r}) = \sum_{g'} \Sigma_{g' \to g, \hat{\Omega}' \to \hat{\Omega}}(\vec{r})\phi_{g'}(\vec{r}) + \frac{\chi_g}{k} \sum_{g'} \Sigma_{fg'}(\vec{r})\phi_{g'}(\vec{r}) \qquad (1.10)$$

Solving the steady-state transport equation (1.10) for a full core is a daunting computational task. After energy, angle and space discretization, writing the neutron balance equation and solving it becomes very complicated. Moreover, from (1.10) it is apparent that the number of unknowns will grow linearly with the number of groups and quadratically with number of dimensions. For larger geometries, the number of unknowns goes into millions [Nichita, 2015], this makes solving the neutron balance equation very onerous [Nichita, 2009]. Thus, for simplicity in computation, the problem is divided into two parts, firstly, the complex neutron balance equation is solved at the lattice cell level, an intermediate set of macro-region-average macroscopic cross sections are generated, and subsequently, these macroscopic cross sections are used in the diffusion equation (A simpler approximation of the neutron transport equation) to find the power distribution of the whole core.

1.2.Neutron Diffusion Equation

The diffusion equation is an approximation of the transport equation, and it has a simpler structure achieved by approximating the neutron current using Fick's law. Fick's law states that there is a directed flow of neutrons (neutron current) from a region of higher (integral) neutron flux to a region of lower (integral) neutron flux. Its mathematical expression is shown in equation (1.11)

$$\vec{J}_g = -D_g \nabla \phi_g \tag{1.11}$$

where $\vec{J}_g$ is the group neutron current, ϕ_g is integral neutron flux and D_g is the diffusion coefficient of condensed energy group g. The gradient operator on the group flux ϕ_g, is oriented along the direction of the neutron flux increase. As the direction of the neutron current is towards the region of lower flux , a negative sign precedes the gradient . Substituting the neutron current and integral fluxes for the macro regions into the equation (1.10) gives the multi-group diffusion equation as shown in equation (1.12)

$$\nabla \cdot [-D_g(r)\nabla \phi_g(r)] + \Sigma_{tg}(r)\phi_g(r) = \sum_{g'} \Sigma_{g' \to g}(r)\phi_{g'}(r) + \frac{\chi_g}{k} \sum_{g'} \Sigma_{fg'}(r)\phi_{g'}(r) \tag{1.12}$$

which simplifies to

$$\begin{aligned} &-\nabla[D_g(r)\nabla \phi_g(r)] + \Sigma_{ag}(r)\phi_g(r) + \Sigma_{s\_loss\_g}(r)\phi_g(r) \\ &= \sum_{g'} \Sigma_{g' \to g}(r)\phi_{g'}(r) + \frac{\chi_g}{k} \sum_{g'} \Sigma_{fg'}(r)\phi_{g'}(r) \end{aligned} \tag{1.13}$$

Equation (1.13) represents the multi-group diffusion equation used for computation of whole core, where the total cross section Σ_{tg} is decomposed to absorption cross section Σ_{ag} and scatting cross section (loss due to scattering of neutrons) $\Sigma_{s\_loss\_g}$ over condensed energy group g. Furthermore, the condensation of cross sections, fluxes and regions reduces the number of unknown from millions to thousands depending on the spatial discretization. This condensation process is across the neutronic properties are called homogenization, which is an averaging process over coarse energy groups and macro-regions.

For production calculations, two energy group are most often used: a fast energy group and a thermal energy group. Neutrons having more energy than 0.625 eV are grouped as fast, and the rest are grouped as thermal [Donnelly, 1996]The wording thermal represents the fact that neutrons in this group is in equilibrium with their ambient energy/temperature. Thermal neutrons are the primary sources of fission. Neutrons from the thermal group are lost to capture, leakage and up-scattering, the last one due to target-nuclei vibrations. However, all the neutrons generated from fission are fast. They are lost from the fast group due to leakage, resonance capture and down scattering. Equation (1.13) transforms to Equation (1.14) for the fast group and (1.15) for the thermal group.

$$\Sigma_{a1}(r)\phi_1(r) + \Sigma_{12}(r)\phi_1(r) = \frac{1}{k}\left(\nu_1\Sigma_{f1}(r)\phi_1(r) + \nu_2\Sigma_{f2}(r)\phi_2(r)\right) + \Sigma_{21}(r)\phi_2(r) + \nabla(D_1(r)\nabla\phi_1(r)) \tag{1.14}$$

$$\Sigma_{21}(r)\phi_2(r) + \Sigma_{a2}(r)\phi_2(r) = \Sigma_{12}(r)\phi_1(r) + \nabla(D_2(r)\nabla\phi_2(r)) \tag{1.15}$$

ϕ_1 and ϕ_2 are the flux for fast and thermal group. Σ_{a1} is the absorption cross-section for the fast group, Σ_{12} is the down-scattering cross section from fast group to thermal group. ν_1 & ν_2 are the average total neutron yield for the fast and thermal group. Σ_{f1} & Σ_{f2} are the fission cross section for fast and thermal group. Σ_{21} is the up-scattering from thermal group to fast group. Σ_{a2} is the absorption cross-section for the thermal group, D_1 and D_2 are the diffusion coefficients for fast and thermal group. All the cross sections used in equation (1.14) and (1.15) are homogenised and dependent on position. k is called the multiplication constant. For a finite geometry, it is k_{eff} and for infinite geometry it is k_∞. In simpler terms, k is the ratio of the production rate of neutrons to the loss rate of neutrons. The following sections give a brief outline of the thesis, stating work carried out during the research.

1.3. Thesis outline

The thesis consists of seven chapters including the current one. A brief description of the content of each chapter is presented in this section.

Chapter 1: Introduction

This chapter contains a description of the type of calculations used for nuclear power plant design and operations, an explanation of neutron transport equation, neutron diffusion equation and Thesis outline.

Chapter 2: Problem Statement

This chapter contains description of typical PHWR lattice cell, the standard homogenization (SH) method, and problems with the SH methodology,

Chapter 3: Progress to date in PHWR Homogenization

In this chapter, a brief description of the previous research in the relevant field is presented. Both techniques related to Superhomogenization factor and discontinuity factor are discussed.

Chapter 4: Method

In this chapter, the definition of Superhomogenization (SPH) factors, Sub-cell homogenization, spatial discretization used for SPH factor generation are discussed. Additionally, this chapter includes a brief introduction to the transport code DRAGON and the diffusion code DONJON. The code structures and data structures are discussed. There is a short discussion on the modules used in the input file.

Chapter 5: Models

This chapter includes the design of the DARGON model for lattice cell calculations and cross section generation. Short description of burnup calculations is presented. The design of the DONJON lattice cell model is presented. Furthermore, in this chapter design of the DRAGON partial core model (reference model) is described. The design of the DONJON partial core models with sub-cell cross sections (with and without SPH factors) and standard homogenization are explained.

Chapter 6: Results and Discussion

In this chapter, explanation of the normalisation of the results to the fission rate is given. Results tables comprised of calculations without SPH factors, with SPH factors and standard homogenization method, are presented. Results are compared and discussed.

Chapter 7: Conclusion and Future Work

This chapter has the summary of the work done during the research, and subsequently, conclusion and future scope of work are stated.

Chapter 2: Problem Statement

2.1.Introduction

The PHWR lattice is square, the pitch is 28.575 cm, but the fuel elements do not follow a rectangular arrangement. Figure 2.1 shows a typical PHWR lattice cell which consists of moderator, calandria tube, pressure tube, fuel bundle, and high temperature and pressure coolant at the centre. A large volume of heavy water moderator surrounds the fuel channel which consists of the fuel bundle, pressure tube and calandria tube the last two being separated by a gas annulus. The fuel bundle consists of thirty-seven fuel pins. The central pin is surrounded by three more rings of fuel pins. The first ring from the centre has six pins, the second and third ring from the centre have twelve and eighteen pins respectively. Each fuel pin is made of a zircaloy tube which contains the natural uranium fuel pellets. The coolant is heavy water with ~99.7 % purity at ~550K. The moderator is also heavy water, but with ~99.9 % purity at 346 K. The pressure tube is an alloy of Zr-Nb 2.5%, and the calandria tube is made of zircaloy. The ratio between the volumes of the moderator to total lattice cell is 0.82, which suggests a significant part of the lattice cell is moderator, and the fuel channel amounts to only 18% of the lattice cell volume. This configuration amplifies the heterogeneity present in the PHWR lattice cell.

2.2.Standard Homogenization

Solving the multigroup neutron transport equation (1.10) for the full core is computationally challenging. To simplify the problem, the detailed geometrical representation of the core is replace with a simplified one, whereby the cross sections are averaged over each lattice cell. This averaging procedure is referred to as standard homogenization, and it is useful in reducing the size of the mathematical problem.

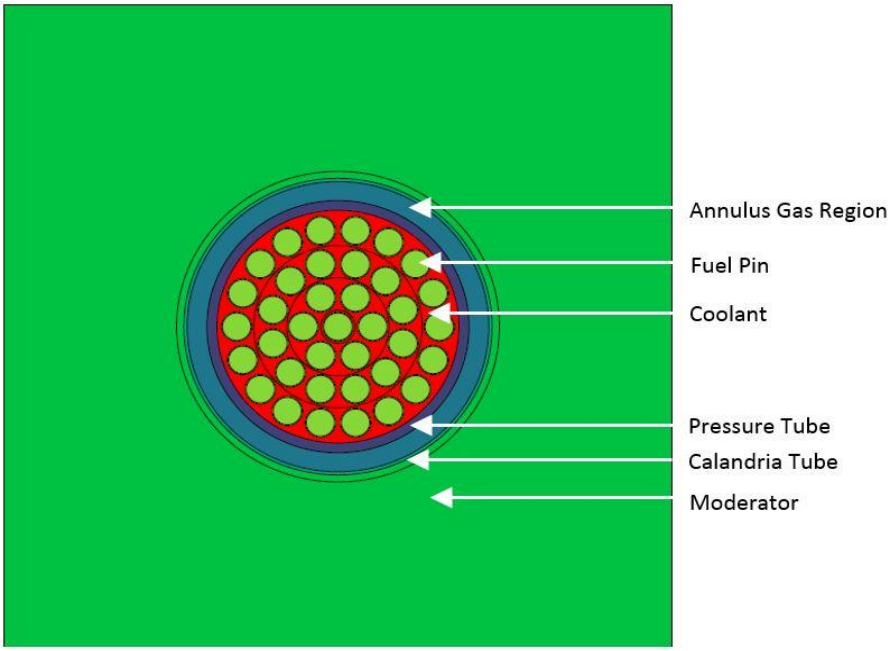

Figure 2.1 A typical 2D PHWR lattice cell.

Subsequently, for full core calculation, the two-group diffusion equations (1.14) and (1.15) are used with the lattice cell-homogenized cross sections. The multi-dimensional, multigroup transport equation is first solved to calculate the cell-homogenized and group-condensed cross sections, using many energy groups (typically more than 50) with a detailed geometrical model for a lattice cell. The average cross sections are then calculated as flux-weighted averages over the lattice cell as shown in equations (2.1) and (2.2).

$$\bar{\phi}_{RG} = \frac{\sum_{r\in R} V_r \sum_{g\in G} \phi_{rg}}{V_R} \tag{2.1}$$

$$\bar{\Sigma}^{x}_{RG} = \frac{\sum_{r\in R}\sum_{g\in G} \Sigma^{x}_{rg}\phi_{rg}V_r}{\bar{\phi}_{RG}V_R} \tag{2.2}$$

$\bar{\phi}_{RG}$ is the average flux over a large region (in this case, one lattice cell) with volume V_R and a coarse energy group G. ϕ_{rg} is flux in a smaller region (calculated to capture neutron behaviors in small regions) with volume V_r and a fine energy group g. $\bar{\Sigma}^x_{RG}$ is a generic, homogenised macroscopic cross section for the large region V_R and coarse energy group G. x can be considered as total or scattering or fission cross sections, Σ^x_{rg} is the generic macroscopic cross section in the small region V_r over the fine energy group g. The error associated with this procedure is mostly due to the heterogeneity present in the large region V_R e.g. solid fuel bundle at the centre and liquid moderator at the peripheral region. Figure 2.2 shows a graphic depiction of the standard homogenization used in PHWR; the different colour represents a different level of the irradiation e.g. freshly fueled channel, channel with mid-burnup and discharge burnup bundles; this is primarily due to daily fueling operations carried out in PHWR operations.

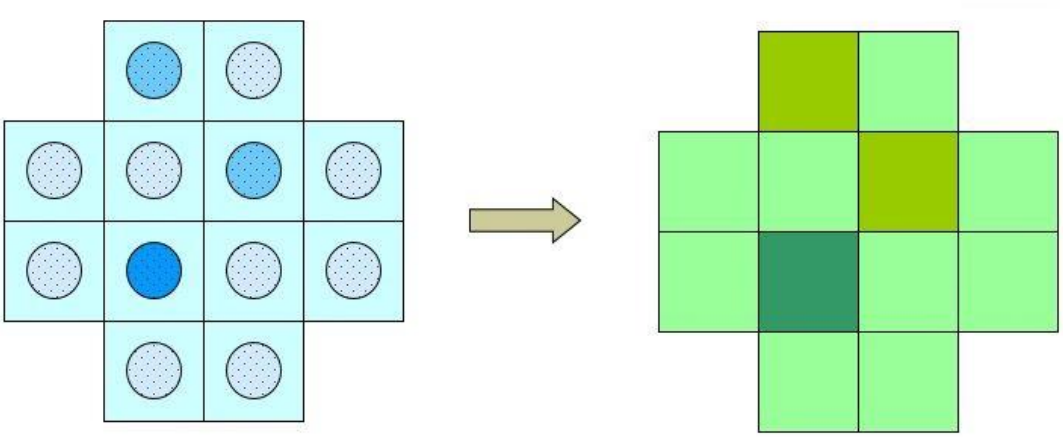

Figure 2.2 Pictorial representation of the standard homogenization method applied in PHWR [Nichita, 2015]

2.3.Problems with Standard Homogenization

In standard homogenization, the transport equation is solved to generate the desired cross section sets for a single lattice cell with reflective boundary conditions, without considering the state of fuel bundles in the adjacent lattice cells, which makes it susceptible to homogenization errors [Shen, 2006]. The replacement of cobalt adjuster rods with stainless steel rods in Pickering A has shown that the homogenised cross sections generated through equation (2.1) and (2.2) do not produce accurate results for strong neutron absorbing materials [Robinson, 1995]. Moreover, the homogenised cross sections generated through the standard homogenization technique could not preserve the reaction rates across the transport and diffusion models. Overall, standard homogenization cannot handle large reactivity changes in small spaces such as may arise due to the presence of a freshly fueled channel adjacent to a channel with high (discharge) burnup fuel [Dall'Osso, 2006]. Furthermore, the presence of large regions of reflector material near the peripheral channels always contributes to inaccuracies in generated cross sections by standard homogenization method.

Chapter 3: Progress to date in PHWR Homogenization

The use of diffusion in conjunction with homogenized macroscopic cross sections obtained using standard homogenization produces less accurate results close to boundaries, neutron sources and neutron absorbers. Finding improved homogenization methods to improve the accuracy of diffusion-theory results has been an active area of reseaerch for the last 40 years. In the case of PWRs, Smith (1980) developed Generalised Equivalence Theory (GET) to address the issue of preservation of reaction rates in both models. In GET the inter lattice leakage is accommodated by making the integral flux discontinuous at the inter lattice boundary. The discontinuity is achieved by multiplying the integral flux by "discontinuity factors". These factors can be generated for both reflective boundary conditions and for proper boundary conditions with leakage representative of the target problem. Assembly Discontinuity Factors are the factors generated when applying GET to PWR fuel assembly with reflective boundary conditions. When proper boundary conditions with leakage are used in GET for the generation of discontinuity factors, these factors are called exact discontinuity factors.

Aragones and Anhert (1986) improved the accuracy of diffusion calculations by setting upan iterative process (using a linear discontinuous finite difference diffusion formulation) to counter the innacuracies of standard homogenization by application of interface flux discontinuity factors.In the diffusion model, they successfully ensured diagonal dominance for the matrices generated by the application of discrete finite difference expansion and spatial discretization by applying limited incremental corrections to the diffusion coefficients. Moreover, this technique led to faster and steady convergence of the eigenvalues in PWR lattice cells surrounded by high reflector boundaries. However, their method needed the incremental corrections calculations to be carried out separately in-between each local and global calculation steps.

Rahnema (1989) generated lattice cell cross sections as a function of boundary conditions with the formulation of boundary condition perturbation theory for improvement in capturing the environmental effects due inter-lattice leakage that may arise due to high differences in burnup between fuel bundles in adjacent channels. Kim and Cho (1993) improved on that by applying a better iterative scheme for generation of lattice cell cross sections with the application of flux weighted constants and variational principles (Pomraning, 1967) for PWR and BWR. They formulated the boundary conditions for fuel assembly cross section generation from both surface flux and leakage calculation using diffusion codes for the full core. Subsequently, they achieved results with similar accuracy by using assembly discontinuity factors (ADF) compared to applying global and local iteration (a computationally intensive method) to their set of PWR problems. Smith (1994) introduced a different method for lattice cell homogenization called "rehomogenization". The homogenised cross sections are generated through recalculation in each step and avoided the adjustment of discontinuity factors in each iteration based on the adjustment of the transport model's net-zero boundary surface current to emulate the flux shape generated by the diffusion model of the whole core. However, the computational process depended on accurate geometry definition of the inter-lattice regions without the advantage of corrections that could have achieved by improving the discontinuity factors in each step.

Rahnema and Nichita (1997) presented a method of corrections of the homogenised cross section and discontinuity factors using a linear interpolation scheme. The interpolation was applied to the homogenised parameters precomputed during the transport calculations. The discontinuity factors and homogenised parameters are independently related to surface current flux ratio at each surface. The technique corrected both the homogenised cross sections and discontinuity factors based on the actual boundary conditions at each lattice cell boundary. This method was successfully applied for the BWR in diffusion theory only, as the approximations used in this method could not handle strong heterogeneity.

Clarno and Adams (2003) computed for environment effect on leakage in the presence of multiple fuel assemblies containing MOX and UO_2 fuel using 1D and 2D models with various configurations. They found encouraging results for fuel assemblies at certain positions in their configurations. Instead of generating discontinuity factors Herrero et al. (2012) developed a function fitting method that incorporates the environmental effects on the computed cross sections. Their method used a simplified Analytic Coarse Mesh Finite Difference (ACMFD) function that eliminated the interacting energy group terms by compensating for them in the cell buckling calculations and yielded a good set of cross sections for pin-by-pin diffusion calculation. Gomes (2012) determined the efficacy of the Assembly Discontinuity Factor (ADF) in the case of highly heterogeneous fuel assemblies with multiple fuel types with different burnups by using finite element codes, he concluded the use of ADF are necessary to get better results in highly heterogeneous configurations in PWR.

Dall'Osso (2006) presented a modified rehmogenization technique, he introduced a delta cross sections coeffeicent to be used with the cross sections generated from the standard homogenization method to account for environmental effects. His methods showed good improvement in preserving reaction rates across the models and showed better estimation of control rod worth. Another innovative technique was applied by Merk and Rohde (2011), in which they introduced reflective boundary condition inside the PWR fuel assembly for transport calculation and analytically solved the two group diffusion equation with an external source on a homogenous 2D model. The technique showed some improvement in efficiency in computation as there was no need of extra iteration compared to methods using discontinuity factors.

One of the important approaches to preserve the reaction rates across the transport and diffusion models is the application of Superhomogenization. Superhomogenization adjusts homogenized cross sections by multiplying them by superhomogenization (SPH) factors (Hebert, 1993) in order

to achieve equality between the reaction rates in the homogenized model and in the heterogenous model. SPH factors address the problems with diffusion models without multiple iterations or modification of the diffusion code. Use of Superhomogenization factor was demonstrated by Hebert (1993) for PWR. It showed promising results in control rod worth measurements against a reference transport model for pin-by-pin homogenization. Superhomogenization (SPH) factors are used with sub-cell (intra fuel assembly) homogenization, which leads to a penalty of additional computation needed due to extra spatial discretization. With the advancement of computing power, the additional computation may not be an issue in future. It is important to notice that Hebert (1993) showed improvements in accuracy for PWR lattice cells, but there was no investigation of PHWR at lattice cell level. Robinson and Tran (1995) used reaction rate conservation technique (similar to SPH method) in the calculation of homogenised cross-sections of stainless steel adjuster rod for Pickering Nuclear power Generating Station. They found some better results compared to standard homogenization technique with respect to actual measurement data of the plant. However, they did not use the technique on PHWR fuel channels. Donnelly, J. V., et al. (1996) discussed the use of SPH factors in reactivity devices measurement in PHWR, they generated 1D (radial) SPH factors for a set of cross section generated in the 2D WIMS-AECL model and used the SPH adjusted cross sections in the RFSP (Reactor Fueling Simulation Program) 3D model to get the reactivity device worth. They were able to get good results for the zone control units only. Results for mechanical absorber rods were having very high errors compared to the actual on-site measurements. However, they did not use 2D SPH factor adjusted cross sections for standard full/partial core calculations with multiple channels and their calculations showed 15% error compared with equivalent DRAGON model.

Berman (2013) pointed out some deficiencies of the SPH application with respect to preserving surface currents. He recommended using surface current adjusted diffusion coefficient to preserve the surface currents. However, SPH factor generation procedure assumes that the boundaries are

all reflective, during the generation of SPH factors the overall buckling is adjusted so that the eigenvalue is reduced to one, which is supposed to account for nonzero surface currents.

Overall, from all the previous works it is evident that there had been a lot of work based on discontinuity factors, and the use of discontinuity factors showed some improvements in LWR computation accuracy, with additional computational steps. There had been some exceptional technique applied to reduce those extra computational expenses but the SPH factors method looks promising because of its ability to circumvent those additional steps of calculations, preserve the reaction rates across the transport and diffusion models and some encouraging results for PWRs discussed by Hebert (2009). Apart from the use of SPH factors in the estimation of the worth of control devices, the method has never been applied in diffusion models in PHWR geometry and thus more investigations of SPH factors in PHWR lattice cell geometry are desirable. The homogenization method described in the present work is based on the use of SPH factors for PHWR lattices, with a specific focus on sub-cell homogenization.

Chapter 4: Method

One possible approach to reduce the errors due to lattice cell homogenization in PHWR is to sub-divide the lattice cell into sub-cells and perform a sub-cell level homogenization. The aim of this research is to investigate the 3 x 3 sub-cell homogenization for a typical PHWR lattice cell using *superhomogenization* (SPH) factors.

4.1. Theoretical background

4.1.1. Sub-cell homogenization

In the standard homogenization method, the homogenised cross sections are generated over the volume of a single lattice cell. Splitting the lattice cell into multiple smaller regions and creating homogenised cross sections for those regions is called sub-cell homogenization. The use of sub-cell homogenised cross section for full core calculation is also referred as heterogeneous diffusion calculations, and superhomogenization factors are used in heterogeneous diffusion calculation to establish equivalency between the transport and diffusion models. In this research, the typical PHWR lattice is divided into nine sub-cell regions in a 3×3 configuration. The eight peripheral regions consist of only the moderator and the central part includes some moderator and the entire fuel channel . Figure 4.1 shows a graphic depiction of the sub-cell homogenization in PHWR. It can be seen that each PHWR fuel channel is divided into nine sub-cell regions. The different colours in figure 4.1 represent various levels of burnup in corresponding lattice cells.

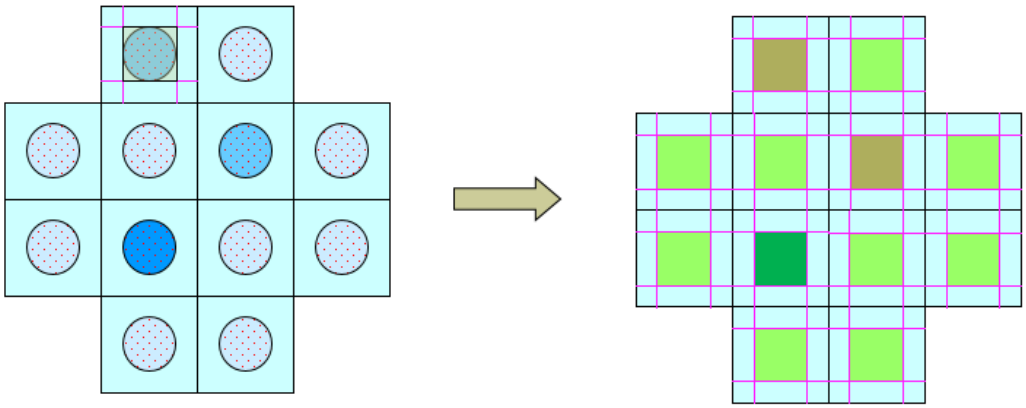

Figure 4.1 Schematic representation of sub-cell homogenization in PHWR fuel channels.

[Nichita, 2015]

4.1.2. Superhomogenization

The diffusion models and the transport models have dissimilarities, which generate different values for the effective multipliction constant for the same geometry and material properties, The superhomogenization (SPH) method is used for establishing the equivalence between the diffusion and the transport models at the sub-cell level. SPH helps to create the equivalence between fine region, fine energy group transport model and coarse region, coarse energy group diffusion model. The equality is achieved by preserving the reaction rates across the models. This equivalence means both the heterogeneous flux $\overline{\Psi}_{RG}$ for coarse region R and group G and diffusion flux $\overline{\Phi}_{RG}$ for same coarse region and the group should yield same reaction rate. For this, the volume and flux weighted cross section $\overline{\Sigma}_{RG}$ for coarse region R and group G has to be multiplied by a factor. That factor is called the SPH factor. The SPH adjusted cross section for coarse region R and group G is defined as

$$\tilde{\Sigma}_{RG} = \mu_{RG} \times \overline{\Sigma}_{RG} \qquad (4.1)$$

where μ_{RG} is SPH factor for coarse region R and group G. The reaction rate is conserved.

$$\overline{\Sigma}_{RG}\overline{\Psi}_{RG} = \widetilde{\overline{\Sigma}}_{RG}\overline{\Phi}_{RG} \tag{4.2}$$

The relationship between the average heterogeneous flux for coarse region R and group G and average diffusion flux for same region and group becomes

$$\overline{\Psi}_{RG} = \mu_{RG} \times \overline{\Phi}_{RG} \tag{4.3}$$

The SPH adjusted cross sections can be substituted to the two energy group diffusion equation (1.14) and (1.15). Equation (4.4) and (4.5) shows the two energy group diffusion equation after the substitution, and subsequently, they are solved for fast flux ϕ_1 and thermal flux ϕ_2.

$$\begin{aligned}\widetilde{\Sigma}_{a1}(r)\phi_1(r) + \widetilde{\Sigma}_{12}(r)\phi_1(r) = \frac{1}{k}\left(\nu_1\widetilde{\Sigma}_{f1}(r)\phi_1(r) + \nu_2\widetilde{\Sigma}_{f2}(r)\phi_2(r)\right) \\ + \widetilde{\Sigma}_{21}(r)\phi_2(r) + \nabla(\widetilde{D}_1(r)\nabla\phi_1(r))\end{aligned} \tag{4.4}$$

$$\widetilde{\Sigma}_{21}(r)\phi_2(r) + \widetilde{\Sigma}_{a2}(r)\phi_2(r) = \widetilde{\Sigma}_{12}(r)\phi_1(r) + \nabla(\widetilde{D}_2(r)\nabla\phi_2(r)) \tag{4.5}$$

For the same geometry and material composition, the fast and thermal fluxes found after solving equation (4.4) and (4.5) are same as the fast and thermal fluxes generated by solving the transport equation (1.10), after normalisation. SPH factors address major issues of diffusion models with standard homogenization as input; SPH adjusted sub-cell cross sections had enabled more accurate total core calculations for PWR [Hebert, 2009].

4.2.Computational Tools

Two standard codes are used for the computational purpose in this research; one is transported code DRAGON [Marleau, 2009], and the other is diffusion code DONJON [Varin, 2005]. Both the codes are developed at École Polytechnique de Montreal and are used in the Canadian nuclear industry to perform lattice cell and full-core calculations. The codes have datatype as linked lists and

functions as modules. They use CLE-2000 language as scripts, and the modules are linked together by the GAN generalised driver, a brief description of the codes is given in this chapter.

4.2.1. DRAGON

DRAGON follows the deterministic approach for solving the integral neutron transport equations; the code can solve the integral neutron transport equation in two ways for a specified geometry. Firstly using 2D and 3D collision probability techniques and secondly by using the method of characteristics. It includes all of the functions that characterise a lattice cell code divided into several calculation modules. The exchange of information between the different modules is ensured by exchange of well-defined data structures. For this study, the collision probability method is used to solve the neutron transport equation for fluxes and multiplication factors (eigenvalues).

The code requires nuclear data from cross-section libraries, geometry information and module definitions for the desired calculation steps. The nuclear data is used to generate the macroscopic cross sections for all materials (mixtures) in the model, while the geometry information defines the fuel assembly structures. For this study a PHWR-lattice-cell geometry was modeled.

4.2.2. DONJON

DONJON is used in the nuclear industry to perform full reactor core diffusion calculations, it has its roots in diffusion solver code TRIVAC-3 and reactor modelling code XSIMUL. The code follows the deterministic approach for solving 2D and 3D multi-group diffusion equation, DONJON includes all the functions to characterise a reactor core. Several calculation modules perform these functions. The modules are linked together by the GAN generalised driver and the exchange of information between the modules is ensured by exchange of well-defined data structures. The code requires the following inputs, like cross section of lattice cells/homogenized volumes, geometry information and module definitions for the desired solution by the developer.

Geometry information primarily defines the fuel assembly/lattice cells and reflector arrangements. For this study, my geometries portray homogenized volumes of PHWR fuel bundles and heavy water moderator. The geometries are divided into several regions and the desired group fluxes and are found by solving the multi-group diffusion equation in each region. There are multiple methods available in DONJON to solve the diffusion equation. In this research, the mesh cornered finite difference method is applied due to the application of sub-cell homogenizations.

4.2.3. DRAGON/DONJON Code-Input Structure

There are three principal parts of the DONJON and DRAGON input. Those are the definition of materials, the definition of geometry and definition of solution control. Some prerequisites and post requisites precede and follow respectively the major parts described above. The prerequisites are declarations of variables and reference to microscopic cross sections library files. The post requisite is the output file design as per the user's requirements. Figure 4.2 represents a typical schematic of the DRAGON/DONJON input structure [Marleau, 2009].

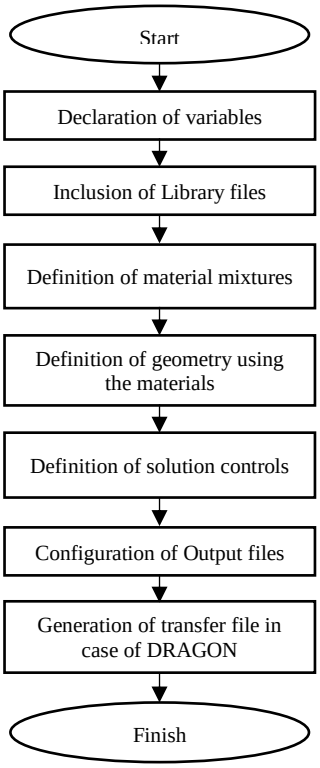

Figure 4.2 Schematic of the input file structure for DRAGON/DONJON

4.2.4. Modules

There are several modules available in the two codes to carry out different functions associated with solving the transport or diffusion equations. Some of the necessary modules used in DARGON are the LIB: GEO: NXT: SHI: ASM: FLU: EDI: and EVO: The LIB: module is used in the inclusion of microscopic library to the definition of material mixtures. The GEO: module is used for geometry definition. The spatial discretization needed for the computational accuracy, and it is applied in the geometry definition. The NXT: module is required to generate the tracking files for the defined geometry. The SHI: module used to capture the self-shielding phenomena on the fuel pin boundary. ASM: module is used for generating the collision probability matrix for the defined geometry. The FLU: module solves the transport equation for the flux and eigenvalues. The EVO: module is used for burnup calculations. EDI: modules gives the user flexibility in generating condensed cross sections for the desired energy levels.

The modules employed by DONJON are GEOD: BIVACT: BIVACA: FLUD: MACD: and OUT: . The GEOD: module is used for geometry definition and additional spatial discretization. MACD: is used for reading the macroscopic cross sections of homogenised sections as a part of the martial definition. BIVACT: and BIVACA: are used for tracking information generation based on the type calculation chosen to solve the diffusion equation in 2D. FLUD: module is used for solving the diffusion equation for the flux and eigenvalues. OUT: module is used for generating output files based on the user requirements.

4.3.Calculation Steps

The following methodology is used for the investigation of the 3 x 3 sub-cell homogenization for a typical PHWR lattice cell using *superhomogenization* (SPH) factors. Firstly, for a PHWR lattice cell, the sub-cell macroscopic cross sections with and without SPH factors are generated using transport code DRAGON and the boundary conditions used in the lattice cell model are reflective.

However, during normal operations, every lattice cell remains critical. To simulate that effect, all the calculation done at the lattice cell level are type B_1 calculations and this calculation method solves the transport equation by adjusting the leakage to ensure criticality at the lattice cell level [Hebert, 2009].

Secondly, these sub-cell cross sections are put in the diffusion model for the lattice cell generated using the diffusion code DONJON. It's important to notice that the diffusion and transport equations are different as previously discussed in section 1.1 and 1.2, therefore, in the solution the eigenvalues and fluxes are different. Subsequently, the fluxes are normalised to the fission rate in both results to observe the equivalency. After the successful equivalency test, further sub-cell macroscopic cross sections both with and without SPH factors and full-cell cross sections (SH) at different burnup level are generated for subsequent use in diffusion models.

A partial core reference DRAGON model is developed, to be used as a reference. This model has nine PHWR lattice cells in a 3×3 configuration. Out of the nine lattice cells, two of the lattice cells have fresh fuel, and the rest have fuel at the discharge burnup level. Equivalent DONJON partial core models are developed and these models are capable of handling both sub-cell (with and without SPH factors) and full cell cross sections. Total fission rate is calculated and normalised to one for each PHWR fuel bundle model, in the next page figure 4.3 shows a brief description of the methodology followed during the research. In the following chapter figure 5.1 and 5.5 shows the lattice cell model developed in the DRAGON and DONJON respectively and the figures for partial core models are shown in section 5.2.

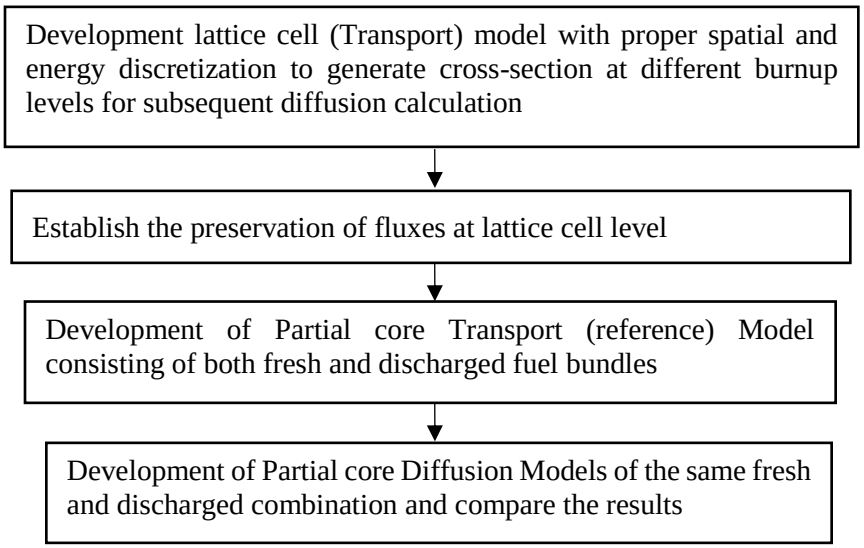

Figure 4.3 Methodology flow chart

4.4.SPH factor generation in DRAGON

There are two major steps for sub-cell SPH factor generation. Firstly, for desired geometry the transport equation is solved using the lattice code DRAGON. The results obtained from the lattice code sets the target reaction rates. Secondly, SPH factors are generated in an iterative process to get the equivalency with target reaction rates established in the first step. Subsequently, the full-core calculations can be performed using the SPH adjusted cross sections and diffusion coefficients. As PHWR fuel bundle is cylindrical, fine Cartesian meshes can't be applied to get the sub-cell SPH adjusted cross sections. DRAGON can generate SPH factors for rectangular geometry only. Therefore, in this research, SPH factors for square and rectangular sub-cell regions are produced.

Chapter 5: Models

This chapter includes a description of the DARGON model for lattice cell calculations and cross section generation. A short description of burnup calculations is also included. A description of the DONJON lattice cell model is presented as well. Furthermore, in this chapter, the description of the DRAGON partial core model (reference model) is described and the design of the DONJON partial core models with sub-cell cross sections (with and without SPH factors) and standard homogenization are explained.

5.1.Lattice Cell Models

There are two lattice cell models, one transport model and one diffusion model. The homogenised macroscopic cross sections for both sub-cell and full cell are generated using DRAGON. The sub-cell cross sections are used in the DONJON (diffusion) lattice cell model. As stated earlier, in this research, the typical PHWR lattice cell is divided into nine sub-cell regions in a 3×3 configuration where the eight peripheral regions consist of only moderator, and the central part includes all components of a typical PHWR lattice cell. The homogenised cross sections and flux distribution are condensed to two energy groups with the group boundary at 0.625 eV. Energies below the 0.625 eV energy level from the thermal group, while those above from the fast group.

The PHWR lattice cell consists of a fuel bundle residing within a pressure tube containing high temperature and high-pressure D_2O coolant (see figure 2.1). The fuel bundle consists of 37 fuel pins arranged in three concentric rings surrounding a central pin. The first ring from the centre has 6 pins while the second and third rings have 12 and 18 pins, respectively. Each fuel pin consists of around 30 UO_2 pellets that are encased by a layer of cladding which is modelled as 100% natural zirconium. The fuel is modelled with a density of 10.6 g/cm^3 and a U-235 weight percent of 0.711 corresponding to natural uranium. A calandria tube surrounds the pressure tube, which in turn is

surrounded by D_2O moderator that is kept thermally isolated from the coolant by the presence of an annular gap between the two tubes. The pressure tube is modelled as an alloy of natural zirconium with 2.5% niobium while the calandria tube is modelled as 100% natural zirconium [Haroon et al., 2016].

5.1.1. DRAGON Lattice cell model

A DRAGON lattice cell model with 3x3 sub-cell splitting is developed. It takes the sub-cell geometry, material mixtures and microscopic cross section libraries as input and generates macroscopic cross sections data of two groups for the full cell as well as the individual sub-cell regions using collision probability method. The microscopic cross section library used, is developed by the WIMS-D Library Update (WLUP) project at the IAEA. The microscopic thermal scattering cross sections for light water and heavy water are taken from the library file using INFO: module in DRAGON. Figure 5.1 shows the single lattice cell DRAGON model utilised in this study. There are some extra splitting in the x and y-axis at the centre of lattice cell model for computational purposes. The lattice cell model also generates the library file and burnup file containing the burned cross sections as well as isotope densities. The DRAGON version used in this research is the 32 bit v-3.05. The lattice cell model is used for the burnup estimation, the desired group fluxes and k_{eff} calculations. Macroscopic cross sections for the entire cell as well as for the sub-cells are generated both with and without SPH factors.

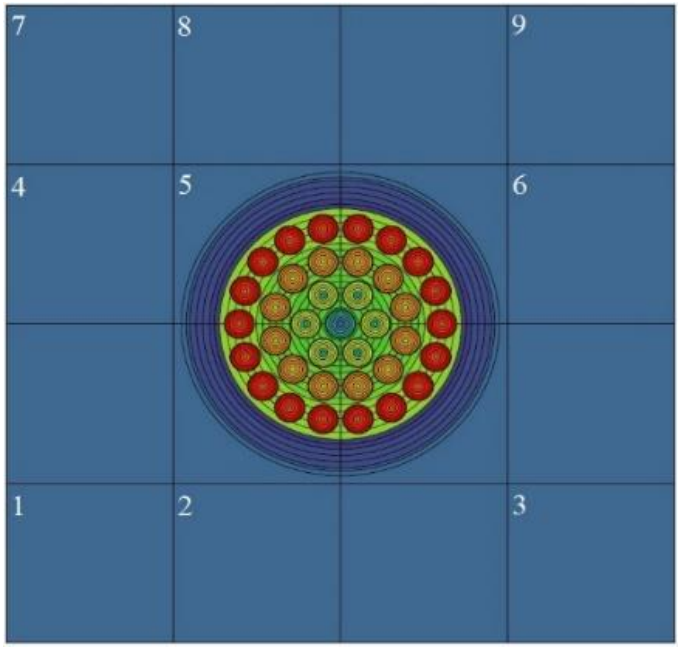

Figure 5.1 PHWR Lattice cell model generated using DARGON 3.05. Colours represent different material mixtures

5.1.1.1. Spatial discretization

The geometry is divided into several regions for adequate spatial discretization. For cylindrical PHWR fuel bundles, Cartesian mesh refinement can not be used, but SPH can be applied by using larger sub-cell divisions, that is why the PHWR lattice cell is split into nine regions in the configuration of 3×3. The coolant region must be divided into annuli of thickness equal to 0.25 to 0.5 times the mean free path of the neutron to model the nuclear interactions accurately and in the case of heavy water, the average mean free path around 2 cm, therefore, for PHWR this corresponds to individual spatial regions with a width of 0.5 cm to 1.00 cm [Jonkmans, 2006]. A 4x4 division is sufficient for the moderator, where the spatial variation of the neutron flux is much slower. Finer spatial discretization at lattice cell levels leads to marginally more accurate results at the expense of computing time. In this research, these practices are applied, and the fuel channel part of the PHWR lattice cell (region 5 in figure 5.1) is divided into 128 regions. Out of the 128 regions, only

4 are rectangular regions and 124 are circular regions in the 2D lattice cell transport model. Overall, the lattice cell is divided into 140 regions. This spatial discretization at PHWR lattice cell level is shown in figure 5.2.

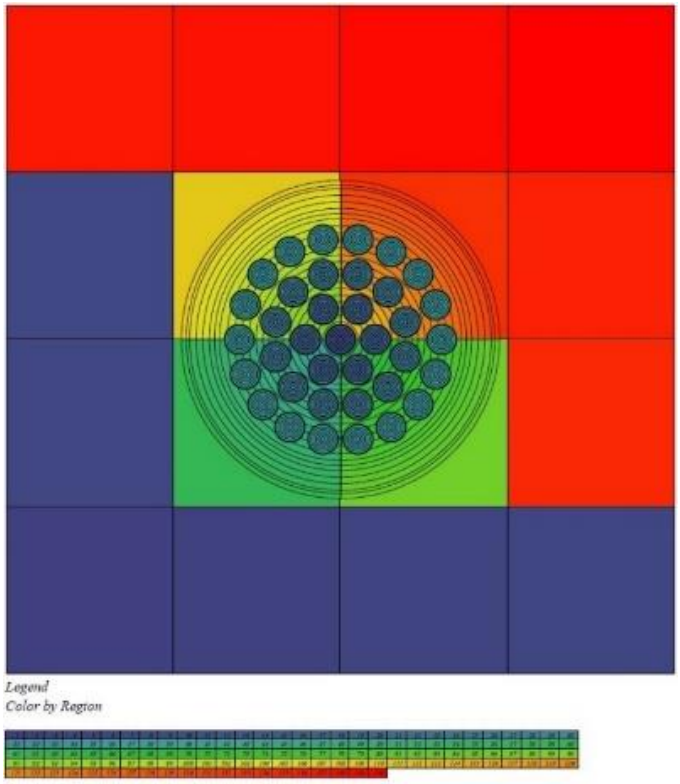

Figure 5.2 Spatial discretization applied in DRAGON lattice cell.

5.1.1.2. Self-shielding Calculations

Material mixture definitions are an essential part of the lattice cell modelling. There is a common practice to use multiple identifiers for the same material composition and this practice helps in avoiding unintended smearing of material compositions spatially distributed across the fuel channel [Jonkmans, 2006]. Figure 5.3 shows a single fuel pin with 8 fine radial spatial regions with 4 material mixtures and out of the 4 material mixtures, 3 are the fuel compositions which is natural uranium dioxide.

Due to neutron absorption in fuel resonances, high localised absorption occurs at the periphery of the fuel pin. These resonance absorptions lead to a lower number of thermalized neutrons reaching the centre of the fuel pin. This phenomenon is called self-shielding, and it is captured by the SHI: module in DRAGON. The use of multiple identifiers for the same fuel composition enables the computation of the loss of neutron due to self-shielding. In the lattice model the fuel at the clad boundary is indexed separately to perform the self-shielding calculations [Marleau, 2009].

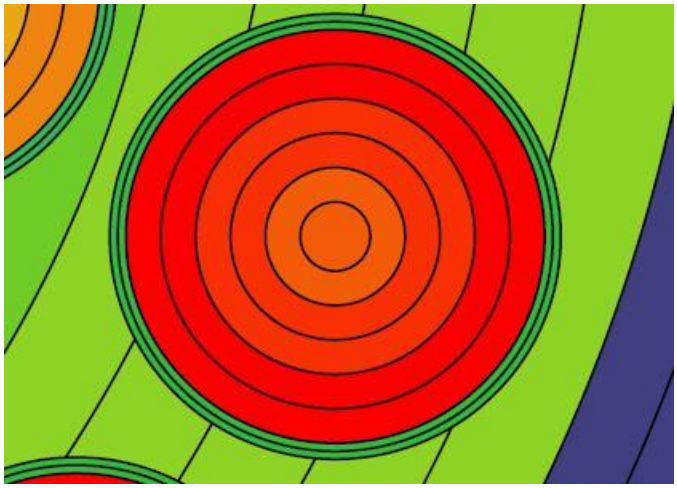

Figure 5.3 Fine spatial discretization at fuel pin level in the lattice cell model.

5.1.1.3. Burnup calculations

The burnup calculation is performed using the EVO: module, using multiple steps to calculate the burnup-dependence of the fuel composition in the lattice cell. For the calculation of the fuel composition beyond fresh-fuel conditions, the lattice cell, is irradiated at a power density of 25 kW/kg (U) with the time step adjusted such that the final burnup of 7,500 MWd/t (U) is reached in twenty burnup steps. Between 0 and 1250 MWd/t(U), the burnup steps range from 25 to 250 MWd/t(U) to capture the initial, sharp decline of the reactivity due to the accumulation of saturating fission products, followed by its subsequent rise resulting from plutonium buildup. Beyond 1250 MWd/t(U), the burnup steps are increased to 375 MWd/t(U) and then to 625 MWd/t(U) between

the mid-burnup value of 3750 MWd/t(U) and the final discharge burnup of 7500 MWd/t(U) [Haroon et al., 2016].

5.1.1.4. Leakage adjustment and output file

The boundary conditions used in the lattice cell model are reflective, corresponding to an infinite lattice. Theoretically, that means the loss of neutrons due to leakage is zero. However, in all real reactors there is always a significant number of neutrons leaking out. During normal, steady-state, operation every lattice cell remains critical. To simulate that effect, all the calculation done at the lattice cell level are type B_1 calculations and this calculation method solves the transport equation by adjusting the buckling to ensure criticality at the lattice cell level. Full cell cross sections and sub-cell cross sections both with and without SPH factors are generated at all burnup levels with the EDI: and BIVACT: modules. Figure 5.4 shows a diagram of the data flow in the lattice cell model used in this research. The final output file consists of results generated by the numerical calculation, plus generic information like the version of the code, title of the input file, and date and time of execution.

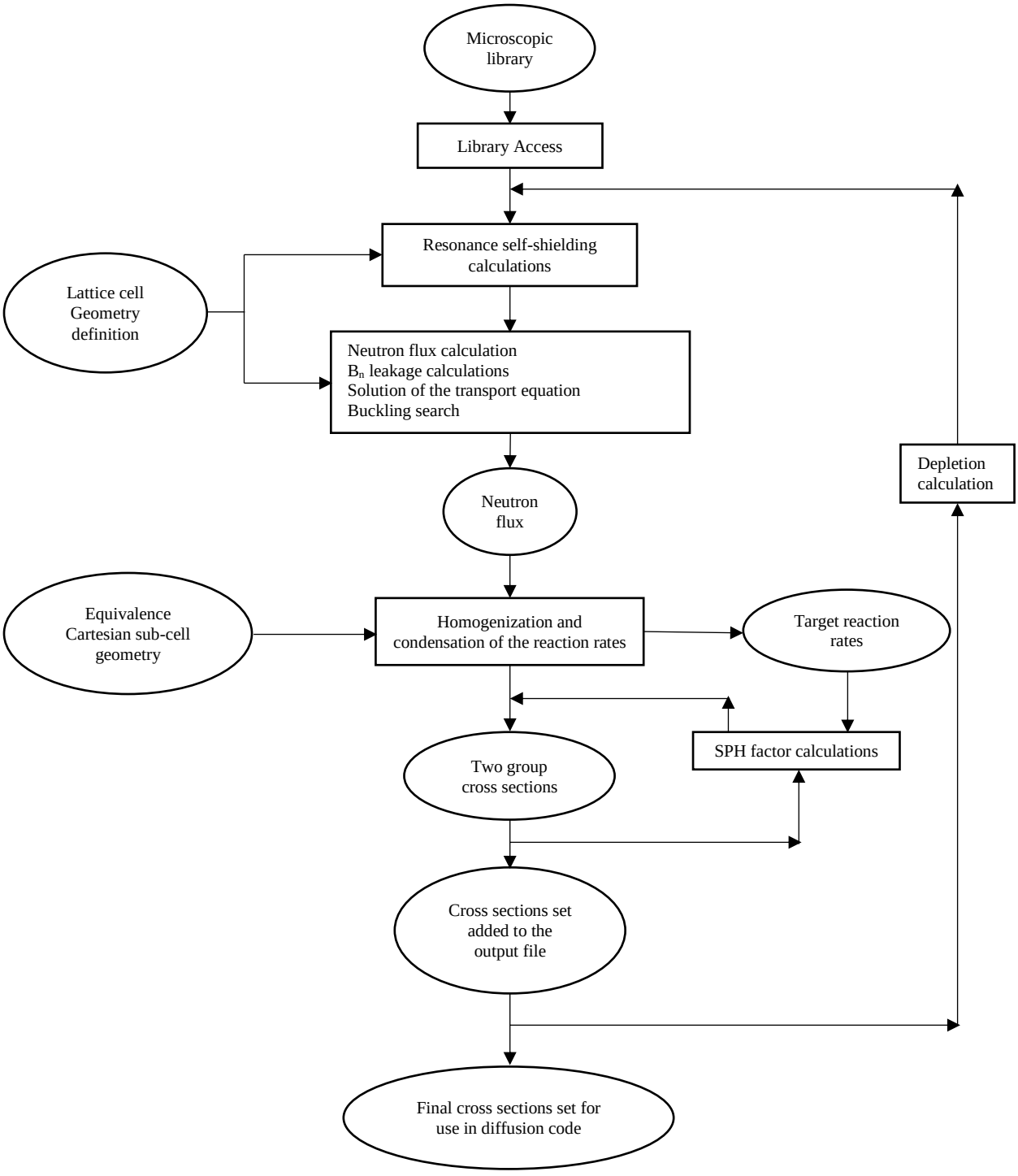

Figure 5.4 Diagram of the data flow in the DRAGON lattice cell model

5.1.2. DONJON lattice cell model

DONJON is used for diffusion calculations. In this study, the sub-cell cross sections generated during the lattice calculations are used to construct a diffusion model of the lattice cell. The aim is to compare lattice-level diffusion results with lattice-level transport results and verify whether the two types of reaction rates are equal. Lattice cell level DONJON models using sub-cell cross sections both with and without SPH factors are developed. Figure 5.5 shows the DONJON lattice cell model.

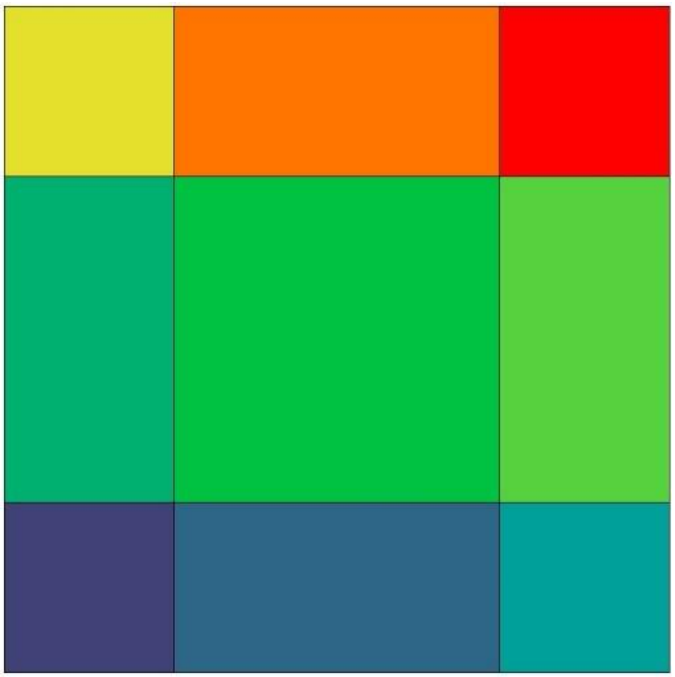

Figure 5.5 DONJON lattice cell model. Each colour represents a different set of homogenized cross sections

5.2.Partial core models

For testing the application of SPH factors, multiple partial core models are developed. All partial core models have nine PHWR lattice cells arranged in a 3×3 configuration. Out of the nine PHWR lattice cells, seven fuel bundles are modelled with discharge burnup level, and two fuel bundles are

modelled as fresh fuel bundles, to add heterogeneity to the partial core models. All the outer boundary conditions are taken to be reflective. The partial core reference model is developed using DRAGON, and the other partial core models are developed using DONJON. Several types of cross sections and discretizations are used for the DONJON models: full-cell cross sections (standard homogenization), sub-cell cross sections with and without SPH factors, and with different spatial discretization (81 and 144 regions).

5.2.1. Reference Partial Core Model

A partial core transport model is developed in DRAGON as a reference for k_∞ and fission rate results. Figure 5.6 shows the reference partial core model; ZB represents zero burnup cross sections, and DB represents discharge burnup cross-sections, which is 7500 MWd/t(U) for a typical PHWR fuel bundle. In the reference model, the nine PHWR lattice cells are divided into 144 major square regions. All fuel channels are split into 1116 annular regions; this detailed spatial discretization is used to improve the accuracy of the reference model. The burnup-dependent cross sections and isotope density files generated in the lattice cell DRAGON model are used as input data to the partial core diffusion model.

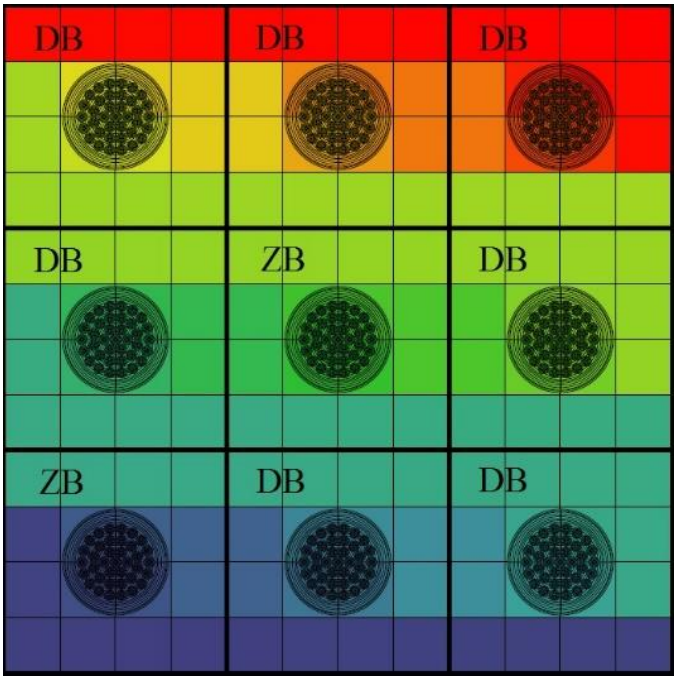

Figure 5.6 3×3 Partial core reference model designed in DRAGON ZB represents zero burnup sections, and DB represents discharge burnup.

5.2.2. Partial Core DONJON Models

There are three DONJON partial core models. The first one uses full cell cross sections of both the depleted and fresh fuel bundles. It is based on the current industry practices of standard homogenization. Figure 5.7 shows the partial core model with standard-homogenization cross sections. The two colours represent two burnup levels; ZB represents zero burnup cross-sections, and DB represents discharge burnup cross-sections.

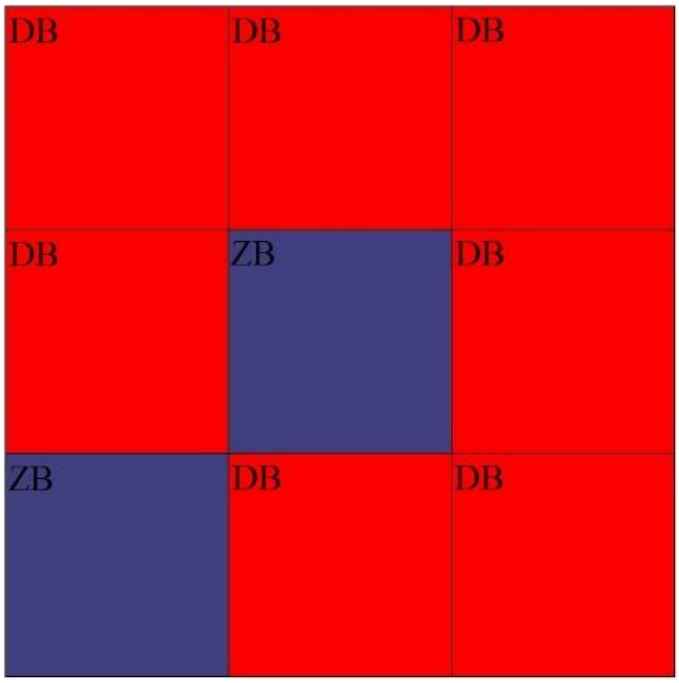

Figure 5.7 Partial core DONJON model with Standard Homogenization. Each colour represents a different set of homogenized cross sections

The other DONJON partial core models use sub-cell cross sections both with and without SPH factors. One of the models has further splitting around the centre of each PHWR channel (for test purposes), with the total number of regions being increased from 81 to 144. Figure 5.8 and Figure 5.9 represent the DONJON partial core models with 81 and 144 regions splitting respectively.

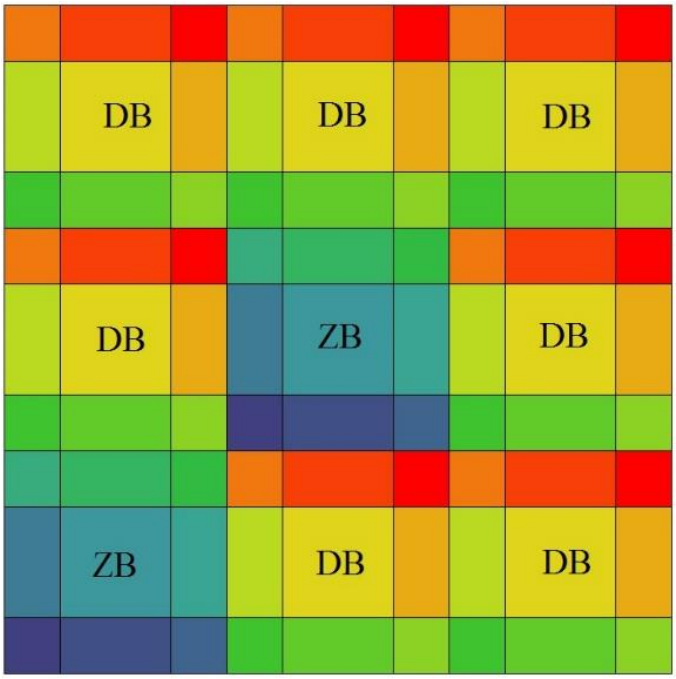

Figure 5.8 DONJON partial core model with sub-cell homogenization with 81 regions. Each colour represents a different set of homogenized cross sections

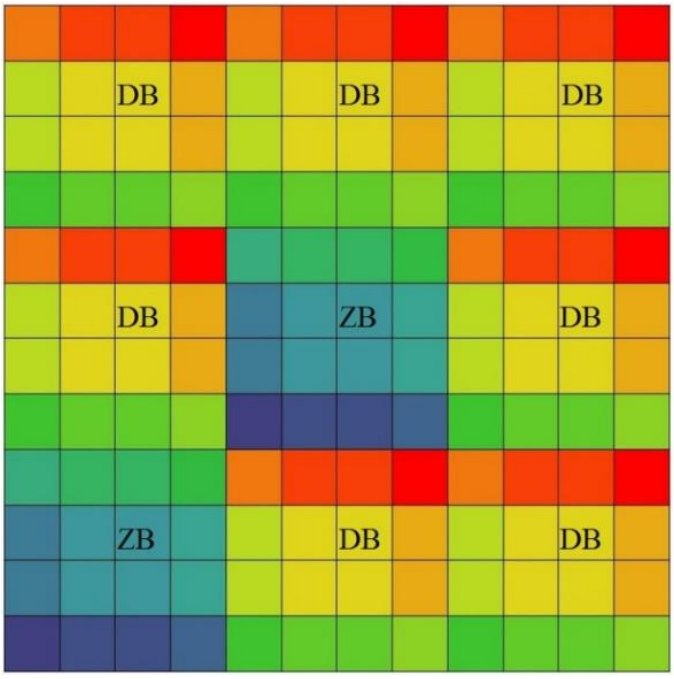

Figure 5.9 DONJON partial core model sub-cell homogenization with 144 regions. Each colour represents a different set of homogenized cross sections

Chapter 6: Results and Discussion

6.1.Flux Normalisation

The neutron balance transport equation and the diffusion equation are eigenvalue problems. Their solutions represent the neutron flux and k_{eff}. The neutron flux being the solution to an eigenvalue problem, it can only be determined up to a multiplicative constant, leaving open the question of its normalisation. In order to perform fair comparisons between results of different eigenvalue problems (such as transport and diffusion), both fluxes have to be normalised the same way. This work normalises all results to a total fission rate of one fission per second (corresponding to ~3.204E-11 watts). The detailed normalisation procedure is shown below.

Let ϕ_{rg} be the average flux for the region r and energy group g and let $\bar{\phi}_{rg}$ be the average flux normalised to a total given fission rate for the region r and energy group g. Then

$$\bar{\phi}_{rg} = C \times \phi_{rg} \tag{6.1}$$

where C is the fission rate normalisation factor which can be adjusted in order to achieve the desired total fission rate, R_0.

Then

$$R_0 = \sum_{r=1}^{R} V_r \left(\sum_{g=1}^{G} \Sigma_{fgr} \times \bar{\phi}_{gr} \right) \tag{6.2}$$

where Vr is the volume of a fine region r. After substituting equation (6.1) in (6.2), the following is obtained

$$R_0 = \sum_{r=1}^{R} V_r \left(\sum_{g=1}^{G} \Sigma_{fgr} \times C \times \phi_{gr} \right) \tag{6.3}$$

As C is independent of region or energy group, one can write:

$$R_0 = C \times \sum_{r=1}^{R} V_r \left(\sum_{g=1}^{G} \Sigma_{fgr} \times \phi_{gr} \right) \tag{6.4}$$

It follows that C can be calculated as:

$$C = \frac{R_0}{\sum_{r=1}^{R} V_r \left(\sum_{g=1}^{G} \Sigma_{fgr} \times \phi_{gr} \right)} \tag{6.5}$$

The normalised average flux $\bar{\phi}_{rg}$ for region r and energy group g is then calculated using equation (6.1) and the value of C determined above. In this work $R_0 = 1$ always.

6.2.Lattice cell results

Tables 6.1 and 6.2 show the lattice cell results for the case without and with SPH factors respectively.

Table 6.1 Normalised fluxes and %error for the lattice cell without using SPH factors (arbitrary units)

Dragon fast flux			Donjon fast flux			%Error in fast flux		
2.30E-01	2.60E-01	2.30E-01	2.46E-01	2.67E-01	2.46E-01	6.70	2.90	6.70
2.60E-01	3.83E-01	2.60E-01	2.67E-01	2.98E-01	2.67E-01	2.90	-22.37	2.90
2.30E-01	2.60E-01	2.30E-01	2.46E-01	2.67E-01	2.46E-01	6.70	2.90	6.70
Dragon thermal flux			Donjon thermal flux			% Error in thermal flux		
6.55E-01	6.23E-01	6.55E-01	5.51E-01	5.22E-01	5.51E-01	-15.90	-16.25	-15.90
6.23E-01	4.71E-01	6.23E-01	5.22E-01	4.80E-01	5.22E-01	-16.25	1.86	-16.25
6.55E-01	6.23E-01	6.55E-01	5.51E-01	5.22E-01	5.51E-01	-15.89	-16.25	-15.89

Table 6.2 Normalised fluxes for the lattice cell with using SPH factors (arbitrary units)

% error is zero in all cases

Dragon fast flux			Donjon fast flux			% Error in fast flux		
2.59E-01	2.81E-01	2.59E-01	2.59E-01	2.81E-01	2.59E-01	0.00	0.00	0.00
2.81E-01	3.13E-01	2.81E-01	2.81E-01	3.13E-01	2.81E-01	0.00	0.00	0.00
2.59E-01	2.81E-01	2.59E-01	2.59E-01	2.81E-01	2.59E-01	0.00	0.00	0.00
Dragon thermal flux			Donjon thermal flux			%Error in thermal flux		
6.22E-01	5.96E-01	6.22E-01	6.22E-01	5.96E-01	6.22E-01	0.00	0.00	0.00
5.96E-01	5.59E-01	5.96E-01	5.96E-01	5.59E-01	5.96E-01	0.00	0.00	0.00
6.22E-01	5.96E-01	6.22E-01	6.22E-01	5.96E-01	6.22E-01	0.00	0.00	0.00

6.3.Lattice cell results interpretation

The sub-cell cross sections are same in both the DRAGON (transport) and DONJON (diffusion) models. Therefore, the conditions of preservation of reaction rates depend on the convergence of fast and thermal fluxes in each model. Sub-cell cross sections with SPH factors and without SPH factors are used in different DONJON models. The results in Table 6.1 are from the DONJON model which uses sub-cell cross sections without SPH factors and the results in Table 6.2 are from the model which uses SPH adjusted sub-cell cross sections. It is evident from the tables that preservation of reaction rates is achieved in the DONJON model in which SPH adjusted sub-cell cross sections are used. The DONJON model without SPH adjusted sub-cell cross sections show an error of 22.37% in Fast fluxes thus the SPH adjusted sub-cell cross sections are found to be useful in lattice-cell level calculations. Moreover, from the tables 6.1 and 6.2 it is also observable that fast and thermal fluxes are symmetric along the corner sub-cells, top-bottom and left and right sub-cells, it is due to symmetricity in the lattice cell geometry. The fact that the diffusion results match the transport results when SPH factors are used, and the fact that the results reflect the symmetry of the geometrical model indicate that both the transport and diffusion models are correct.

6.4.Partial-Core Results

The transport (DRAGON) 3×3 partial-core model is the reference model. The k-eff, fluxes, normalised fission rates found in the reference partial core model is considered absolute and the results found in the DONJON partial core models are compared with respect to the reference model's results. This error in the normalised fission rate is calculated based on the equation 6.7. $Nfission\_rate$ stands for normalised fission rate.

$$\%Error = \frac{Nfission\_rate\_Donjon - Nfission\_rate\_Dragon}{Nfission\_rate\_Dragon} \times 100 \qquad (6.7)$$

The error in the k effective is calculated based on equation 6.8.

$$error = (k\_effective\_Donjon) - (k\_effetive\_Dragon) \qquad (6.8)$$

There are two types of calculations carried out in the reference model. First one is the type B calculations. In this calculations, the leakage is adjusted through a buckling search for criticality conditions. The k-eff becomes 1 and the critical buckling is calculated. The second set of calculation is called type K calculation, in this calculation, the k-eff is calculated without considering the leakage. As all the boundary conditions are reflective the k type calculation, yield a supercritical value for k-eff. All results related to the partial core model is presented in this section. Table 6.3 and Table 6.4 show the k-eff and normalised fission rate of the partial core reference model with type K and type B calculations respectively. The channels at the bottom left and at the centre have the fresh fuel bundles and the rest seven channels have the fuel bundles at the discharge burnup levels. This configuration is chosen so that symmetry in the results can be expected as it is helpful for the result analysis. Table 6.5 represents the results of partial core DONJON model with Standard Homogenization. Table 6.6 and Table 6.7 show the results of the DONJON partial core model for sub-cell homogenization both with and without SPH factors.

Table 6.3 k-eff and normalised fission rates for type K calculations of partial core reference model

k_{eff}	1.01193	
Normalised fission rate		
0.967	0.966	0.953
1.000	1.064	0.966
1.116	1.000	0.967

Table 6.4 k-eff and normalised fission rates for type B calculations of partial core reference model

k_{eff}	1.00000	
Normalised fission rate		
0.967	0.966	0.953
1.000	1.064	0.966
1.117	1.000	0.967

Table 6.5 k-eff and normalised fission rates of partial core DONJON model with standard homogenization.

k_{eff}	0.99983	
Normalised fission rate		
0.985	0.986	0.985
0.992	1.040	0.986
1.049	0.992	0.985

Table 6.6 k-eff and normalised fission rates of partial core DONJON model for sub-cell homogenization (a) with SPH factors (b) without SPH factors for 81 region splitting

(a)

k_{eff}	0.99990	
Normalised fission rate		
0.982	0.984	0.982
0.986	1.054	0.984
1.059	0.986	0.982

(b)

k_{eff}	1.03031	
Normalised fission rate		
0.983	0.985	0.981
0.992	1.043	0.985
1.056	0.992	0.983

Table 6.7 k_{eff} and normalised fission rates of partial core DONJON model for sub-cell homogenization (a) with SPH factors (b) without SPH factors for 144 region splitting

(a)

k_{eff}	0.99034	
Normalised fission rate		
0.981	0.982	0.982
0.983	1.062	0.982
1.064	0.983	0.981

(b)

k_{eff}	1.02016	
Normalised fission rate		
0.982	0.984	0.981
0.989	1.051	0.984
1.059	0.989	0.982

All the results show symmetry around the fresh fuel bundles in the central channel and left bottom channel in the 3×3 configuration. Table 6.8 lists the errors in the k_{eff} and normalised fission rate of the results of DONJON models with respect to the partial core reference model with type k calculations. In Table 6.8, in results of the sub-cell homogenization models with and without SPH factors, the values in the left column represent the error of the DONJON model with 81 regions

and the values in the right column represent the error of the DONJON model with 144 regions. Two fresh fuel channels coloured in cyan and seven fuel channels with fuel at discharge burnup level coloured in magenta. Table 6.9 shows the same set of results as presented in Table 6.8 but in this case, the reference DARGON model has the type B calculations where the leakage is introduced to ensure criticality.

Table 6.8 k-eff and normalised fission rate errors in 81regions and144 regions w.r.t reference model with type K calculations

k-eff Dragon reference	1.01193					
k-eff error in SH	-0.01210					
k-eff error with SPH	-0.01202			-0.02158		
k-eff error without SPH	0.01838			0.00823		
Fission rate in Dragon	0.967		0.966		0.953	
% error in SH	1.89		2.14		3.34	
% error with SPH	1.57	1.44	1.86	1.74	3.05	3.00
% error without SPH	1.63	1.54	1.99	1.89	2.94	2.94
Fission rate in Dragon	1.000		1.064		0.966	
% error in SH	-0.87		-2.28		2.15	
% error with SPH	-1.39	-1.75	-0.95	-0.19	1.87	1.74
% error without SPH	-0.79	-1.15	-2.00	-1.29	1.99	1.89
Fission rate in Dragon	1.117		1.000		0.967	
% error in SH	-6.10		-0.87		1.89	
% error with SPH	-5.15	-4.74	-1.39	-1.75	1.58	1.44
% error without SPH	-5.48	-5.16	-0.78	-1.15	1.64	1.54

Table 6.9 k-eff and normalised fission rate errors in 81regions and144 regions w.r.t reference model with type B calculations

k-eff Dragon reference	1.0000					
k-eff error in SH	-0.00017					
k-eff error with SPH	-0.00010			-0.00966		
k-eff error without SPH	0.03031			0.02016		
Fission rate in Dragon	0.967		0.966		0.953	
% error in SH	1.88		2.13		3.33	
% error with SPH	1.56	1.42	1.85	1.72	3.04	2.99
% error without SPH	1.62	1.52	1.98	1.88	2.93	2.93
Fission rate in Dragon	1.000		1.064		0.966	
% error in SH	-0.87		-2.26		2.14	
% error with SPH	-1.39	-1.76	-0.93	-0.17	1.86	1.73
% error without SPH	-0.79	-1.15	-1.98	-1.27	1.98	1.88
Fission rate in Dragon	1.116		1.000		0.967	
% error in SH	-6.07		-0.87		1.88	
% error with SPH	-5.12	-4.71	-1.39	-1.75	1.56	1.43
% error without SPH	-5.45	-5.12	-0.79	-1.15	1.63	1.53

6.5. Partial-core results interpretation

Both the error tables show similar effects; there is no significant improvement in errors due to the implementation of sub-cell homogenization both with and without SPH factors over the Standard lattice cell Homogenization. In the case of the middle lattice cell in the bottom row and middle lattice cell in the left column, the errors increase after applying sub-cell cross sections with SPH factors. The model with sub-cell cross sections without SPH factors gives good results for 81 regions but in the case of 144 regions the errors increase in some cases. However, the diffusion models with sub-cell cross sections without SPH factors do not have reaction rate equivalence with the transport models at lattice cell level.

6.6. Discussion

The results in Table 6.1 and 6.2 show that use of SPH factors helps in preserving the reaction rates across the diffusion and transport models for single PHWR lattice cell. However, results from the partial core model with nine PHWR lattice cells in 3×3 configuration did not yield any significant advantages over the standard homogenization method. Tables 6.8 and 6.9 show similar homogenization errors in the case of standard homogenization and sub-cell homogenization with SPH factors. This demonstrates the limited effectiveness of sub-cell homogenization with SPH factors.

From the table 6.8, the k-eff has the error of 12.1mk in the case of the Standard Homogenization as this method could not handle configurations where the heterogeneity is high because of side by side fresh and discharge fuel bundles (Chapter 2). The maximum error of 21mk is observable in the case of the DONJON model with 144 regions and SPH factors whereas in the case of sub-cell homogenization without SPH factors the error in k-eff reduces. The minimum error in the k-eff is 8.1mk and observed with DONJON model with 144 regions splitting without using SPH factors; this shows the inefficiency of the SPH factors in handling additional spatial discretization.

The errors in normalised fission rates for the fuel channels in the middle of the bottom row and the middle of the left column increases compared to the errors from standard homogenization. In the case of DONJON model constituting of the sub-cell cross sections without SPH factors for 81 regions, the results are better than the standard homogenization. However, it is already demonstrated in section 6.2 that at lattice cell level the sub-cell cross sections without SPH factors don't preserve the reaction rates with the transport model. Furthermore, the addition of extra spatial discretization and increasing the number of regions to 144 in the same DONJON model without SPH factors increases the errors in some channels. This result indicates the opposite behaviour in the diffusion model for PHWR, as in the case of transport models increase of spatial discretization

always leads to improved results. Therefore, the use of sub-cell cross sections without SPH factors may not result in better outcomes in case of PHWR.

The likely explanation is the SPH factors calculated in the single lattice cell transport model differ from the SPH factors found in the 3×3 partial core transport model. Table 6.10 shows the error in the thermal SPH factors calculated in 81 regions in the partial core model with respect to the SPH factors calculated in single lattice cell model. The left bottom fuel channel has the maximum error in the thermal SPH factors, and the normalised fission rate error in the same channel is also maximum. Similarly, the second highest error in normalised fission rate is in the right top row; the same fuel channel also has the second largest error in thermal SPH factors. This one to one error relations between the fuel channels shows the dependence of error in normalised fission rate with errors in thermal SPH factors.

Table 6.10 Percentage error in thermal SPH factors in partial core model (81 regions) with respect to single lattice model.

2.33	2.34	2.38	2.47	2.74	3.12	3.44	3.79	4.04
1.84	1.84	1.82	1.83	2.12	2.57	3.03	3.50	3.79
1.07	1.03	0.79	0.57	0.96	1.47	2.23	3.02	3.43
0.24	0.12	-0.29	-0.34	-0.09	0.74	1.47	2.57	3.12
-1.44	-1.39	-1.60	-1.63	-1.27	-0.09	0.95	2.12	2.74
-3.47	-3.17	-3.08	-2.51	-1.63	-0.34	0.56	1.82	2.46
-4.89	-4.42	-3.63	-3.09	-1.60	-0.29	0.78	1.82	2.38
-6.36	-5.73	-4.43	-3.17	-1.39	0.11	1.03	1.84	2.33
-7.23	-6.36	-4.90	-3.48	-1.45	0.23	1.06	1.83	2.32

On the other hand, the boundary condition in partial core model is reflective, that eliminates the effect of leakage at the edge of the model, moreover, discharge fuel has less fissile material and more fission products that absorb neutrons and fresh fuel has more fissile material and fewer fission products. Moreover, due to the presence of fresh and discharge fuel side by side, high heterogeneity

is generated, which affects the neutron leakage at inter-lattice boundaries. No other parameter has changed between the conditions of the single lattice cell model and partial core model except the inter-lattice leakage, therefore the errors in SPH factors can be attributed to the inter-lattice leakage rate at the partial core model. This effects also makes the SPH factors depend on the positions of the fresh fuel bundles and discharge fuel bundles.

Overall, from the results, it's observable that the SPH factors work well in single lattice cell model but, their effect in multiple lattice cell model is not significant. Application of SPH factors in the 3×3 partial core model did not yield any good results. The SPH factors can't handle the heterogeneity in the partial core model as they depend on the position of the lattice cells with different burnups in the partial core model. That reduces the use of SPH factors for full-core calculations with the traditional two-stage computational scheme in the PHWR.

Chapter 7: Summary, Conclusion and Future Work

7.1. Summary

In this research, the use of Superhomogenization factors for sub-cell homogenization of PHWR lattice cell is investigated. The PHWR lattice cell is large and strongly heterogeneous, which leads to homogenization errors when applying full-cell homogenization. One possible method to reduce those errors is to sub-divide the lattice cell into sub-cells and perform sub-cell-level homogenization. In this study, the PHWR lattice cell is divided into 3 x 3 sub-cells. The eight peripheral regions consist of only the moderator, and the central part includes all components of a typical PHWR lattice cell but, due to the sub-cell division, its size is reduced to 14.28cm×14.28cm. A lattice cell model with the desired sub-cell division is developed using the lattice code DRAGON. Full-cell, as well as sub-cell two-group cross-sections, are generated for subsequent use in an equivalent two group two-dimensional DONJON (diffusion) model.

In nominal states, the reactors are operated at criticality, for this reason, to simulate steady state operation at lattice cell level all cross sections are generated using a B_1 leakage model. For the sub-cell homogenization, one set of cross sections are generated using the *superhomogenization* approach which uses additional parameters called *superhomogenization* (SPH) factors and other sets of sub-cell cross sections are generated without the SPH factors to demonstrate the efficacy of the SPH methods.

After the successful application of SPH factors at the lattice cell level, the effect of using SPH adjusted sub-cell homogenization is tested on partial core models consisting of 3 x 3 lattice cells (bundles), some of which have zero-burnup, and rest have discharge-burnup fuel. The results from the transport (DRAGON) partial core model are compared with the results from diffusion (DONJON) partial core models obtained using full-cell homogenization (SH) and sub-cell homogenization both with and without SPH factors.

7.2.Conclusion

From Table 6.8, it is observable that the error in the k-eff is maximum in case of the DONJON model with 144 regions and SPH factors. In the case of error in the normalised fission rate, results from the two lattice cells are worse than the standard homogenization method, one of them is the channel in the middle of the bottom row, and the other is the middle channel of the left column. These results show that the use of SPH adjusted sub-cell homogenization does not produce any significant improvement over the Standard Homogenization method when applied to PHWR lattice cell using a 3×3 sub-cell division. The SPH factors depend on the position of the region in a model with multiple PHWR lattice cells. This outcome is due to the effect of leakage at the inter-lattice boundary. Further investigation with finer splits at the lattice cell boundary might improve the results.

7.3.Future Work

SPH factors depend on the position of the region in case of models with multiple PHWR lattice cells, as they do not address heterogeneity due to different burnup levels. On the other hand, the biggest advantage of SPH factor is the ease of implementation through any diffusion code without needing any modifications. Using finer spatial discretization at lattice cell boundaries for SPH factors generation might improve the results. This research also showed that SPH factors could be computed in models with multiple lattice cells, this technique can be used to generate the SPH factors for models with multiple lattice cells (2×2 lattice cells or 3×3 lattice cells) with different heterogeneous configurations, and these results can be used to constitute a diffusion model for the full core. Another application might be using SPH factors (based on 2D geometry) for calculation of incremental cross section of reactivity devices. This application might be the simplest use of SPH factors as most of the models used for determination of incremental cross sections use all the fuel bundles at mid-burnup level. This homogenous burnup level in all lattice cells eliminates any

chance to heterogeneity that might affect the SPH factors, which have already been proven to be good at persevering reaction rates across the transport and diffusion models.

References

1. Aragonés, J. M., & Ahnert, C. "A linear discontinuous finite difference formulation for synthetic coarse-mesh few-group diffusion calculations." Nuclear Science and Engineering 94.4 (1986): 309-322.
2. Berman, Y. "An improved homogenization technique for pin-by-pin diffusion calculations." Annals of Nuclear Energy 53 (2013): 238-243.
3. Clarno, K. T., & Adams, M. L. "Capturing the effects of unlike neighbors in single-assembly calculations." Nuclear science and engineering149.2 (2005): 182-196.
4. Dall'Osso, A. "A spatial rehomogenization method in nodal calculations." Annals of Nuclear Energy 33.10 (2006): 869-877.
5. Donnelly, J. V., Min, B. J., Carruthers, E. V., and Tsang, K. "Modeling of CANDU reactivity devices with WIMS-AECL/MULTICELL and superhomogenization." Proceedings of the 17th Annual Conference of the Canadian Nuclear Society, CNS, Fredricton. 1996.
6. Gomes, G. "Importance of Assembly Discontinuity Factors In Simulating Reactor Cores Containing Highly Heterogeneous Fuel Assemblies." Proc. of COMSOL Conference 2011.
7. Haroon, J., Kicka, L., Mohapatra, S., Nichita, E., and Schwanke, P. "Comparison of the Reactivity Effects Calculated by DRAGON and Serpent for a PHWR 37-element Fuel Bundle." Journal of Nuclear Engineering and Radiation Science.
8. Hebert, A. "A consistent technique for the pin-by-pin homogenization of a pressurized water reactor assembly." Nuclear Science and Engineering 113.3 (1993): 227-238.
9. Hebert, A. Applied reactor physics. Presses inter Polytechnique, 2009.

10. Herrero, J. J., García-Herranz, N., Cuervo, D., and Ahnert, C. "Neighborhood-corrected interface discontinuity factors for multi-group pin-by-pin diffusion calculations for LWR." Annals of Nuclear Energy 46 (2012): 106-115.
11. Jonkmans, G. "WIMS-AECL version 3.1 User's Manual." ISTP-05-5115, IST Product, Protected COG RandD, Atomic Energy of Canada Ltd (2006 June).
12. Kim, H. R., and Cho, N. Z. "Global/local iterative methods for equivalent diffusion theory parameters in nodal calculation." Annals of Nuclear Energy 20.11 (1993): 767-783.
13. Marleau, G., Hébert, A., and Roy, R. "A User Guide for DRAGON, Release 3.05 E." Ecole Polytechnique de Montréal, Montréal, Canada (2009).
14. Merk, B., and Rohde, U. "An analytical solution for the consideration of the effect of adjacent fuel elements." Annals of Nuclear Energy 38.11 (2011): 2428-2440.
15. Mohapatra, S., and Nichita, E. "Investigation of Sub-Cell Homogenization Model for PHWR Lattice Cells using SPH Factors", 40th Annual CNS/CAN student conference, June 19 - 21,Toronto, ON, Canada, 2016.
16. Nichita, E., and Rahnema, F. "A heterogeneous finite element method in diffusion theory." Annals of Nuclear Energy 30.3 (2003): 317-347.
17. Nichita, E., "Inexpensive Detailed Full-Core Neutron Flux Solution Method for CANDU Reactors." Transactions of the American Nuclear Society 100 (2009): 631-633.
18. Nichita, E., "Evaluating accuracy of standard homogenization and need for generalized equivalence theory for ACR®-lattice checkerboard configurations." Annals of Nuclear Energy 36.6 (2009): 760-766.
19. Nichita, E., "Computational challenges in reactor physics." Lecture notes of Special Topics: Modeling and Simulation (NUCL 5005G-005), 2015, FESNS, UOIT, Oshawa.
20. Nichita, E., Partial-Cell Homogenization Progress Report, Queens University, 2015.

21. Pomraning, G. C. "Variational principle for eigenvalue equations." Journal of Mathematical Physics 8.1 (1967): 149-158.
22. Rahnema, F. "Boundary condition perturbation theory for use in spatial homogenization methods." Nuclear Science and Engineering 102.2 (1989): 183-190.
23. Rahnema, F., and Nichita, E. M. "Leakage corrected spatial (assembly) homogenization technique." Annals of Nuclear Energy 24.6 (1997): 477-488.
24. Robinson, R. C., and Tran, F. "Calculation of homogenized Pickering NGS stainless steel adjuster rod neutron cross-sections using conservation of reaction rates." 16th Annual CNS conference, June 4 - 7, Saskaton, SK, Canada, 1995.
25. Smith, K. S. "Spatial homogenization methods for light water reactor analysis." Diss. Massachusetts Institute of Technology, 1980.
26. Smith, K. S. "Practical and efficient iterative method for LWR fuel assembly homogenization." Transactions of the American Nuclear Society71.CONF-941102--(1994).
27. Shen, W. "Development of a multi-cell methodology to account for heterogeneous core effects in the core-analysis diffusion code." Proceeding of The International Conference on the Advances in Nuclear Analysis and Simulation, PHYSOR-2006, Vancouver, Canada. 2006.
28. Varin, E., Hébert, A., Roy, R., and Koclas, J. "A user guide for DONJON version 3.01." Ecole Polytechnique de Montréal, Montréal, Canada (2005).